Energy & Buildings 174 (2018) 147–155

Contents lists available at ScienceDirect

Energy & Buildings

journal homepage: www.elsevier.com/locate/enbuild

Bio-based insulation materials and their hygrothermal performance in a building envelope system (ETICS)

M. Palumbo[a,*], A.M. Lacasta[b], M.P. Giraldo[b,c,1], L. Haurie[b], E. Correal[c,1]

[a] Department of Chemical Engineering, Universitat Rovira i Virgili, Av. Països Catalans, 26, Tarragona 43007, Spain
[b] Barcelona School of Building Construction (EPSEB), Universitat Politècnica de Catalunya, Av. Doctor Marañon 44, Barcelona 08028, Spain
[c] Catalan Institute of Wood, Forest Sciences Centre of Catalonia, Parc de Gardeny, Ed. H2 planta Baixa, Lleida 25003, Spain

ARTICLE INFO

Article history:
Received 7 November 2017
Revised 18 June 2018
Accepted 21 June 2018

Keywords:
Bio-based materials
Bio aggregates
Thermal insulation
Hygrothermal performance
Corn pith
Construction

ABSTRACT

Bio-based insulation materials (such as wood or hemp) are emerging as a promising alternative in building envelope applications, aiming at improving in-use energy efficiency. When compared to common insulation materials (rock and glass wool or petrol-based foams) bio-based materials present the advantage of being renewable, with a low embodied energy and CO_2 neutral or negative. Moreover, these materials have a distinct hygrothermal performance, as the sorption/desorption of water vapour in their porous structure, in dynamic equilibrium with their surrounding environment, constantly modifies their hygric and thermal properties while causing energy transfers itself. In this paper, the hygrothermal performance of two different bio-based materials in outdoor conditions is evaluated. The first is an innovative lightweight composite made from corn pith and alginate. The second a commercially available wood insulator. The materials are tested alone and as components of external thermal insulation systems (ETICS) and compared to a conventional polystyrene foam. The results show how the sorption process influence the hygrothermal performance of the materials when the surrounding conditions are modified. When subjected to cyclic changes in temperature and relative humidity, the bio-based materials tested show a lower temperature variation than polystyrene. This is in part due to their lower thermal diffusivity, but also to the water absorption and desorption mechanisms occurring within the materials, which were measured by the change in mass of the materials during the tests. The differences in the thermal performance were more noticeable when the insulation materials were tested alone than when these were tested as a part of an ETIC System.

© 2018 Elsevier B.V. All rights reserved.

1. Introduction

Recent developments support the use of natural fibres, such as wood, hemp, kenaf, cotton, flax or sheep's wool, as an alternative to thermal insulations based on non-renewable resources. As a result, some bio-based insulation materials such as hemp wools or wood fibres can nowadays be found in the market. Much research has been carried out as well on the use of crop by-products such as straw, stalks or husks of cereals in building applications [9], although such research more rarely resulted in commercial products. Among the available crop by-products, vegetable pith is a promising one [4,16,17]. Pith refers to the parenchymal tissue (or a mixture of parenchymal tissue and spare vascular bunches) of some plants when it forms an elastic, spongy structure. This occurs, for instance, at the inner part of the maize, miscanthus, cattail or sunflower stalks.

The use of bio-based materials for the building insulation purposes has multiple advantages. In addition of being renewable materials with a lower embodied energy than the petrol-based alternatives, their high hygroscopicity provides them with interesting properties for both indoor and outdoor applications [8,9]. Hygroscopic materials have the capacity of adsorbing and desorbing water vapour, which contributes to moderate extremes of humidity in indoor environments [11,12,18,21]. To evaluate this capacity, a useful index, the *Moisture Buffering Value* (MBV), was developed at the NORDTEST Project [19,20]. MBV refers to the mass of water vapour adsorbed and desorbed in the porous structure of a material that is exposed to a surrounding in which the relative humidity is cyclically changed between two levels. In a previous paper [12], the MBV was determined for several experimental and commercial bio-based insulation materials, according to the protocol of the standard ISO 24353 (relative humidity of 73% and 53% for periods of 12 h, at constant temperature of 23 °C). All the

* Corresponding author.
E-mail address: mariana.palumbo@upc.edu (M. Palumbo).
[1] Headquarters: CTFC, Ctra. Sant Llorenç de Morunys, km 2. 25280, Solsona, Espanya.

https://doi.org/10.1016/j.enbuild.2018.06.042
0378-7788/© 2018 Elsevier B.V. All rights reserved.

analysed bio-based materials showed a MBV higher than 1.0 g/m^{2}ΔRH, which correspond to "good" and "excellent" moisture buffers [2], although significant differences were observed among them.

Moreover, a change in the amount of water vapour present in the pores of a hygroscopic material will result in an alteration of its thermal and hygric properties [1,3,5–7,10]. Moreover, sorption processes involve the release (or absorption) of an energy of about 2.5 kJ/g. This heat diffuses through the sample leading to significant variations in temperature. In the previous paper already mentioned [12] samples were tested in environments with constant temperature but cyclic variations of RH. It was found that mass changes in about 2 g lead to variations in temperature inside the sample. When measured at a depth of 15 mm from the exposed surface, such variation was around 2 °C. The results were corroborated by numerical simulations. At higher environmental temperature and/or lower relative humidity, the water vapour content is lower. That means that if temperature increases (RH decreases) some energy needs to be absorbed in order to release the water molecules adsorbed at the surface. The opposite occurs if temperature decreases (RH increases), with the release of some amount of energy. This behaviour is especially relevant when the bio-based insulation is applied at the external side of the building envelope. The external insulation material can be subjected to important daily variations of temperature and relative humidity. For a fixed absolute humidity, a simultaneous increase of temperature and decrease of RH will take place during the day, whereas a simultaneous decrease of temperature and increase of relative humidity will happen at night. In these conditions, the energy absorbed during the heating period (when desorption occurs) and released during the cooling period (when adsorption occurs) will delay the thermic dynamics, thus increasing the thermal inertia.

In this paper, some of the bio-based insulation materials previously analysed for indoor conditions [12] are now tested under variable conditions that are representative of an outdoor environment, that is, simultaneous changes of temperature and relative humidity. The study includes commercial wood fibre (WF) and wood wool (WW) and experimental panels made with corn pith and sodium alginate (CA) [12–15]. Results are compared with those obtained for a conventional polystyrene insulation (EPS). Moreover, as the insulation materials in buildings are integrated into a complex construction system composed of layers of coating materials, the configuration of which determines the service performance of the materials, the hygrothermal performance of three complete *External Thermal Insulation Composite Systems* (ETICS) is also evaluated.

2. Materials and experimental methods

2.1. Materials and samples

Both commercial and experimental insulations materials were tested. The experimental materials were formulated with corn pith and sodium alginate. The pith was removed from corn stalks, ground, and sieved to form a granulate. Samples of two different densities were prepared. The low density one (CA_LD) was made with pith granulate of a particle size of 2 mm, bound with a very low percentage of sodium alginate. The high density one (CA_HD) contained pith particles of smaller size (0.5 mm) and a higher amount of binder. Compositions are shown in Table 1.

The study included other commercially available insulation boards. Two of them were also bio-based materials, as they were made of wood fibres: a flexible low-density wood wool (WW) and a rigid high-density wood fibre board (WF). A non-bio-based insulation, a rigid expanded polystyrene (EPS), was also considered.

First, small samples of dimensions 240 × 160 × 70 mm^3 were prepared in order to measure the thermal properties and analyse the hygrothermal behaviour in dynamic conditions of the materials. Afterwards, three complete thermal insulation systems of 700 × 700 mm^2 were made, each one comprising two layers of the thermal insulator and a render consisting of a flexible mortar system. In the case of the bio-based materials, the two layers of insulation consisted of a first layer of 50 mm of a low-density board and a second layer of 20 mm of a higher density board. The first layer was constructed with a rigid wooden frame, while the second was screwed on top of it. In the case of the EPS, the two layers had the same density. The mortar system was formulated with cement and had three distinct coats: a first one of reinforcing mortar incorporating an imbedded reinforcing fiberglass mesh (2–3 mm), a primer coat, and a render (1–2 mm). A schema of the systems is presented in Fig. 1. The relevant properties of the distinct layers are presented in Table 2.

2.2. Dynamic Vapour Sorption (DVS)

Sorption/desorption measurements were performed using a Dynamic Vapour Sorption analyser DVS-100 (Surface Measurement Systems, UK) equipped with a microbalance. The samples, with a mass of the order of 1 g, were initially dried for 2 h to establish the dry mass. RH humidity was then increased, linearly, from 0 to 90% in 12 h and decreased from 90% to 0% in 12 h. Four cycles were repeated for each sample. Temperature was fixed to 25 °C.

2.3. Thermal properties

The thermal conductivity (λ) and diffusivity (α) were measured using a Quickline-30 Electronic Thermal Properties Analyser (based on ASTM D5930 standard) with a surface probe. Such equipment is based on the analysis of the transient temperature response of the material to heat flow variations induced by electrical heating using a resistor heater having direct thermal contact with the surface of the sample. The measurements were made at room conditions (20 °C; 50%) in triplicate.

2.4. Dynamic hygrothermal test for the insulation boards

The hygrothermal behaviour of the materials were investigated with dynamic tests. A set up was designed where one specimen of each material (CA_LD, WW, EPS) was introduced in a climatic chamber pre-set to fulfil cycles in which temperature and relative humidity shifted. The dimensions of the three samples were of 240 × 160 × 70 mm, and each one was equipped with two thermocouples. One of the thermocouples was placed at the centre of one of the large surfaces of the samples. The other was placed at the center of their inner section (at 35 mm from the large faces). The temperature was recorded each minute. With the aim to minimise the thermal bridge from the sensor cable, a small diameter flexible thermocouple cable was used, and the joint was sealed at the surface with a tape to ensure air tightness. Each experiment was performed twice: a first time in which the temperature was recorded, and a second time in which the thermocouples were removed, and the samples were placed on top of a scale that recorded their weight during the test at a precision of 0.01 g. The two measurements were done separately because of the low density of the samples, which resulted in an important distortion from the sensor cables. The experimental set up is depicted in Fig. 2.

In the experiments, the variation of temperature and relative humidity were constrained in order to maintain a constant absolute humidity in the chamber. The temperature was varied every 12 h, abruptly, from 15 °C to 30 °C while the relative humidity was

Table 1
Composition of the experimental corn pith-alginate samples. The values are presented as % in weight.

Sample	Particle size (mm)	Corn-pith (%)	Alginate (%)	Density (kg/m^3)
CA_LD	2	97.1	2.9	60
CA_HD	0.5	95.0	5.0	100

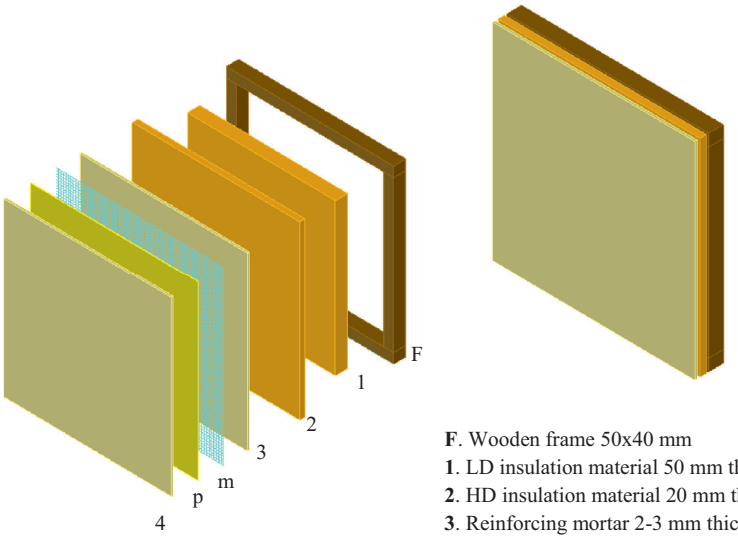


Fig. 1. Schema of the ETICS incorporating bio-based insulations prepared for the tests. In the case of the EPS, layers 1 and 2 had the same density (LD).

Table 2
Main characteristics of the different layers composing the ETIC systems.

ETIC system	Layer	Board type	Composition	Thickness (mm)	Density (kg/m^3)
Corn pith	1	Rigid	CA_LD: Corn pith + sodium alginate	50	60
	2	Rigid	CA_HD: Corn pith + sodium alginate	22	100
	3*	Rigid	Mortar (commercial)	2–3	1400
	4*	Rigid	Render (commercial)	1–2	1800
Wood	1	Flexible	WW: Wood wool, adhesive (commercial)	50	55
	2	Rigid	WF: Wood fibre, adhesive (commercial)	22	230
	3*	Rigid	Mortar (commercial)	2–3	1400
	4*	Rigid	Render (commercial)	1–2	1800
Polystyrene	1	Rigid	EPS: Expanded polystyrene (commercial)	50	30
	2	Rigid	EPS: Expanded polystyrene (commercial)	20	30
	3*	Rigid	Mortar (commercial)	2–3	1400
	4*	Rigid	Render (commercial)	1–2	1800

* Layers 3 and 4 were the same in all three prototypes.

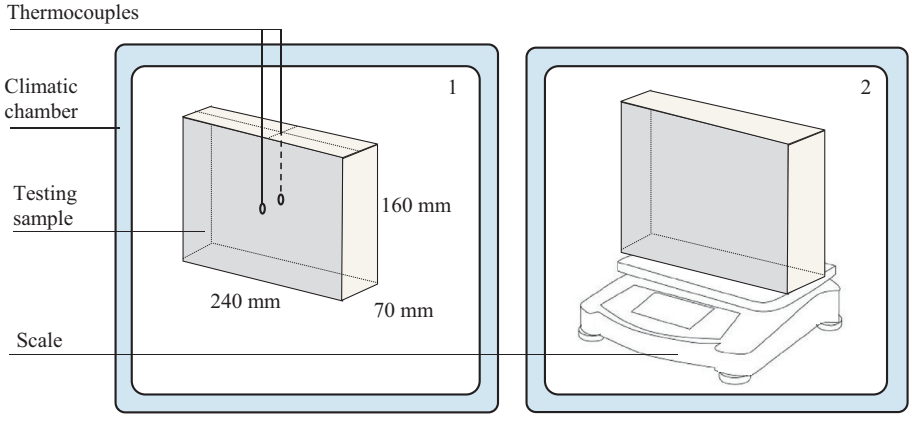


Fig. 2. Schema of the experimental set up.

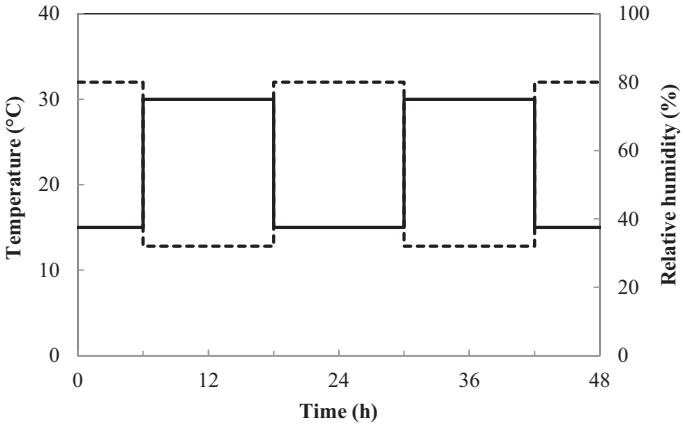


Fig. 3. Schema of the run performed. Solid line correspond to temperature and dotted line to relative humidity.

changed from 80% to 32%, as depicted in Fig. 3. Before each experiment, the samples were conditioned for 24 h at the initial conditions of the run.

2.5. Stationary thermic test for the ETIC systems

In the stationary test, the ETIC systems, of dimensions of 700 × 700 mm, were subjected to a constant temperature gradient. To this end, the samples fitted in the opening of a climatic chamber with the rendered face inside the cooler enclosure and closed up in behind by a highly isolated box. The temperature of the box depended on the heating and cooling system of the laboratory, but the isolation of the box provided stable conditions to the prototype. The temperatures were maintained at 12 °C in the climatic chamber and 32 °C in the isolated box.

Heat flux through the system was measured by attaching a heat flux sensor Hukseflux HFP01 in the free surface of layer 1 (face inside the hotter box). The sensor was attached using a double-sided removable carpet laying tape, in order to avoid any air gap between the sample and sensor surfaces. The uncertainty of calibration of the apparatus was ±3%. The thermal resistance of the sensor was 0.0071 m^2K/W, which was considered to be negligible as it was 2 orders of magnitude lower than the resistances of the samples.

The temperature was recorded at various positions: air temperature within the isolated box (Tai), temperature at the surface of the prototype facing inside the isolated box (Tsi), temperature inside the system, at the interface between the two insulation layers (Tint), temperature at the surface of the prototype facing towards the climate chamber (Tse) and air temperature inside the climate chamber (Tae). Two thermocouples were used for each position, and the average was considered. The experimental set up is depicted in Fig. 4.

2.6. Dynamic hygrothermal test for ETIC systems

In the dynamic test, the prototypes of ETICS were attached at the opening of a climatic chamber, so that one side faced the interior of the chamber and the other side, the testing room. The runs simulated outdoor conditions at the interior of the chamber and indoor conditions at the testing room. Thus, the coated surface of the prototypes was exposed to the interior of the chamber in all the experiments. Heat flux and temperatures were registered similarly as previously described for the stationary test: laboratory air temperature (Tai), surface temperature at the face outside the chamber (Tsi), temperature at the interior of the system, at the interface between the two insulation layers (Tint), surface temperature at the face inside the chamber (Tse) and air temperature inside the chamber (Tae). The position of the sensors was the same as the previously depicted in Fig. 4.

Each run was built by six identical cycles that emulated an average spring day in a moderate climate (CSa, following the Köppen-Geiger classification). Each cycle lasted 24 h, in which the temperature progressively changed from 15 °C to 30 °C and the relative humidity, from 80% to 32%, similar to what would occur in a real evolution of outdoor conditions (Fig. 5).

3. Results and discussion

3.1. Dynamic Vapour Sorption (DVS)

Sorption/desorption measurements were made, as described in Section 2.2, for small samples of corn pith (CA_LD), wood wool (WW) and polystyrene (EPS). It is worth noting that the protocol, consisting of a linear increment of the relative humidity from 0 to 90% (and further linear decrement) is not the standard way of obtaining the sorption isotherms. In a standard run, relative humidity is increased in 5% RH steps up to a maximum of 95% RH, and then decreased to 0% RH in 5% RH steps. The instrument maintains the sample at a constant RH until the weight change is very small. This procedure, even for very small samples, takes many days. Larger scale samples, under real climatic conditions, hardly reach an equilibrium stage, and therefore transient sorption isotherms can be more useful in this study.

In Fig. 6, the moisture content evolution for the three materials is presented. Only two of the four cycles performed are shown. The two natural materials start to adsorb water vapour from the beginning, reaching values of about 15% (Wood wool) and 35% (corn pith) at the maximum RH (90%). Polystyrene does not adsorb water until a time when RH is high enough (about 80%). This water is adsorbed very rapidly at the beginning (until a moisture content of about 4%) and then more slowly up to about 7%. In all the cases, an asymmetry can be seen between the rise and descent curves. This is better shown in the transient sorption isotherms (Fig. 7), where moisture content is plotted versus RH. The hysteresis between the adsorption (solid lines) and desorption (dashed lines) has a maximum of about 2% in the three cases. The vertical lines of Fig. 7 indicate the range of HR considered in the rest of the tests of this work, that is, 32% and 80%. It is interesting to note that, within this range, the variations in moisture content are about 15% for CA, 7% for WW and 5% for EPS.

3.2. Thermal properties

Table 3 summarizes the thermal properties obtained for the analysed materials. The experimental corn-alginate insulations (CA_LD and CA_HD) have values similar to those obtained for wood wool (WW). As expected, the denser wood fibre board (WF) presents a remarkable higher thermal conductivity and a lower diffusivity. EPS may seem to be the best option because of its lower conductivity value. However, its diffusivity value is more than twice higher than the one obtained for the CA and wood materials. To better quantify the importance of diffusivity in thermal dynamics, Table 3 also includes the thermal penetration depth d_p at a time of 10 min, calculated as $d_p = (\pi \alpha t)^{1/2}$, where α is the diffusivity and t the time. Results indicate that, if an increment of temperature is applied to one side of a sample, the depth to which the temperature will change significantly 10 min later is between 26 and 38 mm for the natural materials and 63 mm for the EPS. Therefore, it is expected that EPS will respond more quickly (the order or two times faster) to temperature variations.

According to the thermal conductivities showed in Table 3, and taking into account the thicknesses of the layers composing the

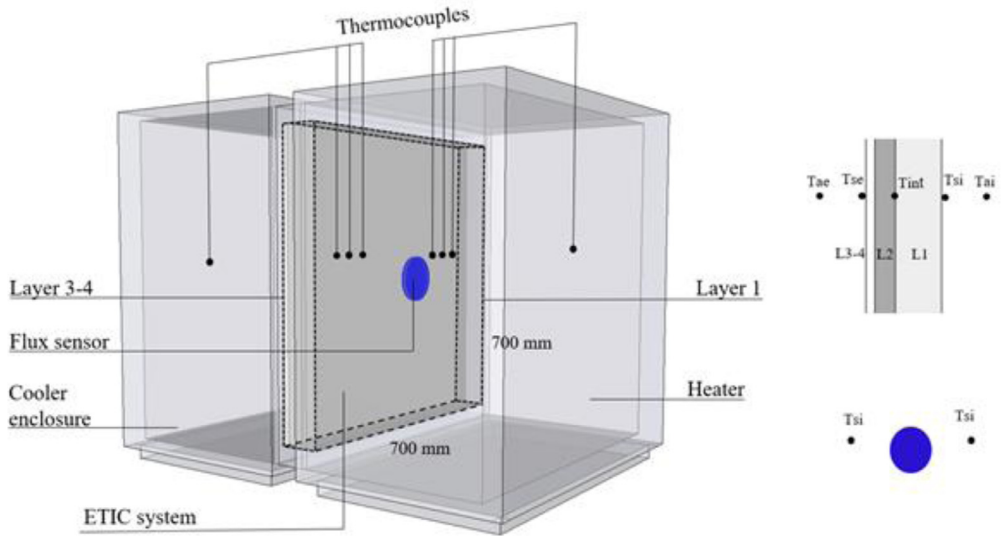


Fig. 4. Schema of the experimental setup.

Table 3
Thermal conductivity, diffusivity, and penetration depth of the insulation materials.

	Thermal conductivity (W/mK)	Thermal diffusivity (10^{-6} m^2/s)	Penetration depth (mm)
CA_LD	0.042 ± 0.001	0.70 ± 0.05	36 ± 1
CA_HD	0.048 ± 0.001	0.65 ± 0.05	35 ± 1
WW	0.047 ± 0.001	0.76 ± 0.05	38 ± 1
WF	0.065 ± 0.001	0.37 ± 0.01	26 ± 1
EPS	0.036 ± 0.001	2,1 ± 0.1	63 ± 1

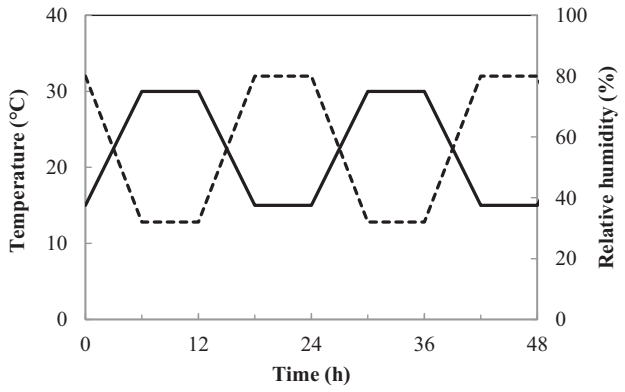


Fig. 5. Schema of the run performed. Solid line corresponds to temperature and dotted line to relative humidity.

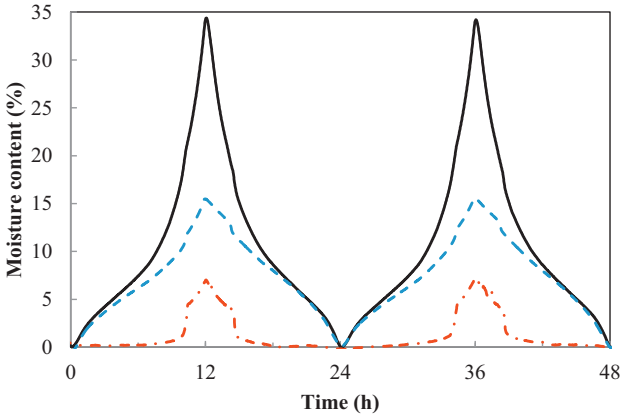


Fig. 6. Moisture content (%) evolution for two cycles of 24 h: CA (black solid line), WW (blue dashed line) and EPS (red dot-dashed line). (For interpretation of the references to colour in this figure legend, the reader is referred to the web version of this article.)

ETIC systems (see Table 2), the thermal resistances and the global thermal transmittance U of the insulation systems can be determined. The U-values of the systems were estimated supposing that the R-values of the layers 3 and 4 (mortar and render) are negligible and considering a thermal resistance of 0.13 m^2K/W for both the interior and the exterior surfaces of the climatic chamber. This value corresponds to the internal surface resistance (R_{si}) described at UNE-EN ISO 6946:2012 standard and was chosen as it was considered that at the experiment set-up, the air movement nearby both surfaces was low. Results are shown in Table 4.

3.3. Dynamic hygrothermal behaviour of insulation boards

The hygrothermal performance of the samples were analysed using the methodology described in Section 2. Three specimens, one of each material (corn pith_LD, wood_wool and polystyrene) were tested in a climate chamber.

The results are depicted in Fig. 8. As expected, the polystyrene sample has a very fast response to the external variations, reaching the chamber temperature in a short time. On the other hand, the hygroscopic characteristics of the two bio-based materials lead to an important slowdown in their thermal dynamics. It is interesting to observe the differences between them. The inset of Fig. 8 shows a zoom for the first two hours of the test. It is possible to observe that the temperature inside the EPS sample grows faster than the other cases, in agreement with its higher diffusivity and depth penetration values (Table 3). The sample incorporating polystyrene reaches 20 °C in only 8 min, whereas corn pith and wood samples

Table 4
Calculated thermal resistances and transmittances of the ETICS systems.

ETIC system	Thermal resistance layer 1 R_1(m^2K/W)	Thermal resistance layer 2 R_2(m^2K/W)	Transmittance U (W/ m^2K)
Corn pith	1.19	0.46	0.52
Wood	1.06	0.34	0.60
Polystyrene	1.39	0.56	0.45

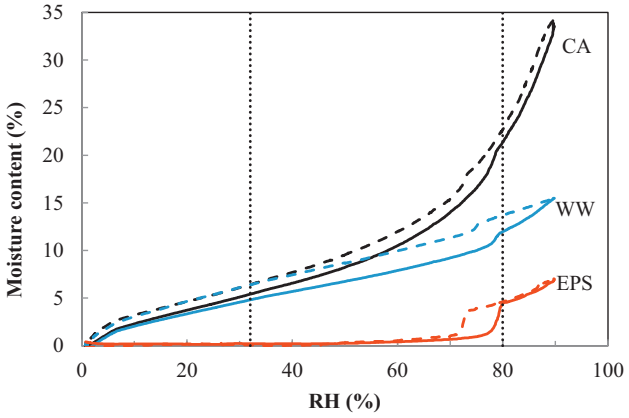


Fig. 7. Transient sorption isotherms for CA, WW and EPS for adsorption (solid lines) and desorption (dashed lines). Vertical lines point the range of HR considered in the rest of the paper (between 32% and 80%).

need about 18 min. At that time, the wood sample starts a plateau that keeps the temperature below 22 °C for two hours. The temperature at the interior of the corn pith sample continues growing until a remarkable slowdown, which occurs at about 25 °C. At time t = 12 h, both the polystyrene and the wood samples have temperatures close to that of the chamber, but the temperature at the corn pith sample is 3 °C lower. A similar behaviour is observed during the cooling process, when external conditions are abruptly changed to 15 °C and 80% RH, although here the plateau for the wood sample is not so clearly observed.

The temperature evolutions are directly related with the absorption and desorption of water vapour and therefore with the mass variations of the samples. In Fig. 9, the temperature at the core of the materials (solid lines) and the mass change (dashed lines) are simultaneously plotted for the three samples. It can be observed that mass variations in the polystyrene sample are minimal. Compared with the corn pith, mass change at the wood material is a bit faster at the beginning, but it slows down after 2 h. After 12 h, corn pith has not reached a stationary mass value yet. This behaviour is in qualitative agreement with the results obtained for dynamic vapour sorption already discussed in Section 2.2. EPS absorbs less quantity of water vapour than the bio-based materials. In addition, the low water vapour permeability of EPS constrains the sorption process to the surface of the sample.

The variations of temperature and mass are more gradual for the bio-based insulation boards due to the higher thermal inertia and hygrothermal behaviour of these lignocellulosic materials. In the case of corn pith, the variations are smoother, and the time needed to reach the stationary state is higher than for wood, probably due to differences in the mechanisms of water absorption and desorption.

3.4. Stationary thermic test for the ETIC systems

Previous to the dynamical study of the ETIC systems, the stationary test described in Section 2.5 was performed on the prototypes of dimensions 700 × 700 mm (see Table 2). Constant temperatures of about 12 °C and 32 °C were maintained in the enclosures at the two sides of each prototype for one week. Table 5 summarize the data, averaged along 2 d, obtained after the stationary regime was achieved. As expected, the wood system showed the highest heat flux value and the polystyrene system, the lowest. From these data, thermal resistances and transmittances can be determined as: Rsi = (Tai-Tsi) / H; R1 = (Tsi-Tint) / H; R2 = (Tint-Tse) / H; Rse = (Tse-Tae) / H and U = H / (Tai-Tae). The results, shown in Table 6, are in good agreement with those presented in Table 4, calculated from the characteristics of each layer of the systems.

3.5. Dynamic hygrothermic test for the ETIC systems

The ETIC system prototypes were tested in a climatic chamber, following the setup and protocol described in Section 2.6.

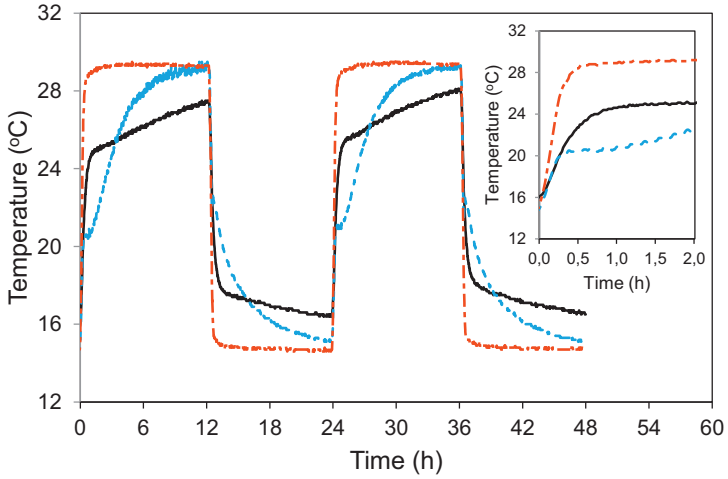


Fig. 8. Temperature registered by the thermocouple placed at the center of the samples: corn pith (black solid line), wood (blue dashed line) and polystyrene (red dot-dashed line) for two cycles of run 2. Inset: zoom showing the first two hours of the heating process. (For interpretation of the references to colour in this figure legend, the reader is referred to the web version of this article.)

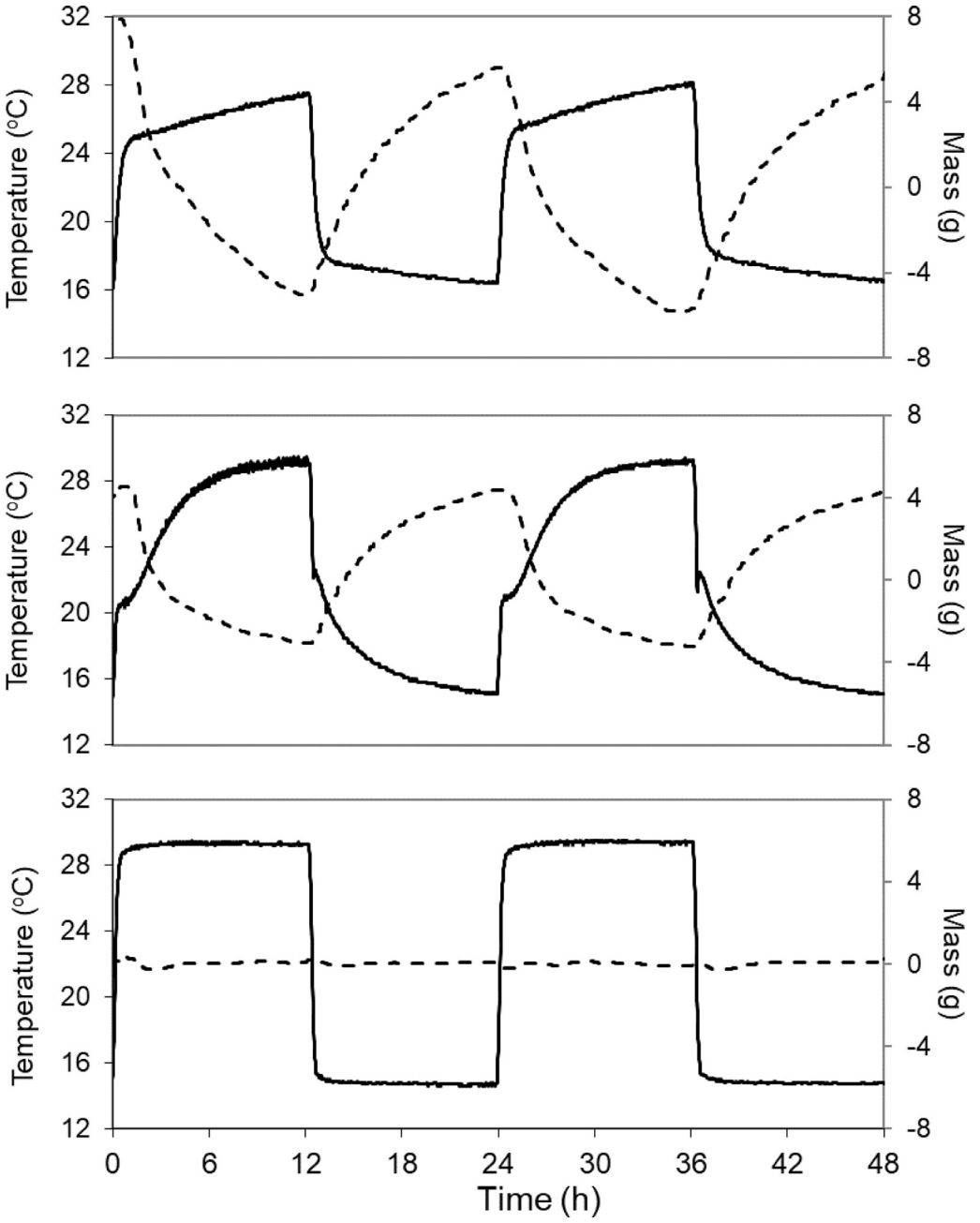


Fig. 9. Simultaneous evolution of temperature at the core of the material (solid lines) and mass (dashed lines) for corn pith (top), wood (middle) and polystyrene (bottom) corresponding to the same cases of Fig. 8.

Table 5
Heat flux and temperatures for the stationary test.

ETIC system	Heat flux H (W/m^2)	Air inner temperature Tai (°C)	Surface inner temperature Tsi (°C)	Interfase temperature Tint (°C)	Surface external temperature Tse (°C)	Air external temperature Tae (°C)
Corn pith	10.6	32.0	30.4	18.4	13.6	12.0
Wood	12.8	32.2	29.0	17.3	12.9	11.3
Polystyrene	8.75	31.2	29.9	18.1	12.9	11.7

Table 6
Measured thermal resistances and transmission of the ETICS.

ETIC system	Internal surface resistance Rsi (m2K/W)	Thermal resistance layer 1 R1 (m2K/W)	Thermal resistance layer 2 R2 (m2K/W)	External surface resistance Rse (m2K/W)	Transmittance U (W/m2K)
Corn pith	0.15	1.13	0.45	0.15	0.53
Wood	0.25	0.92	0.34	0.12	0.61
Polystyrene	0.15	1.35	0.59	0.14	0.45

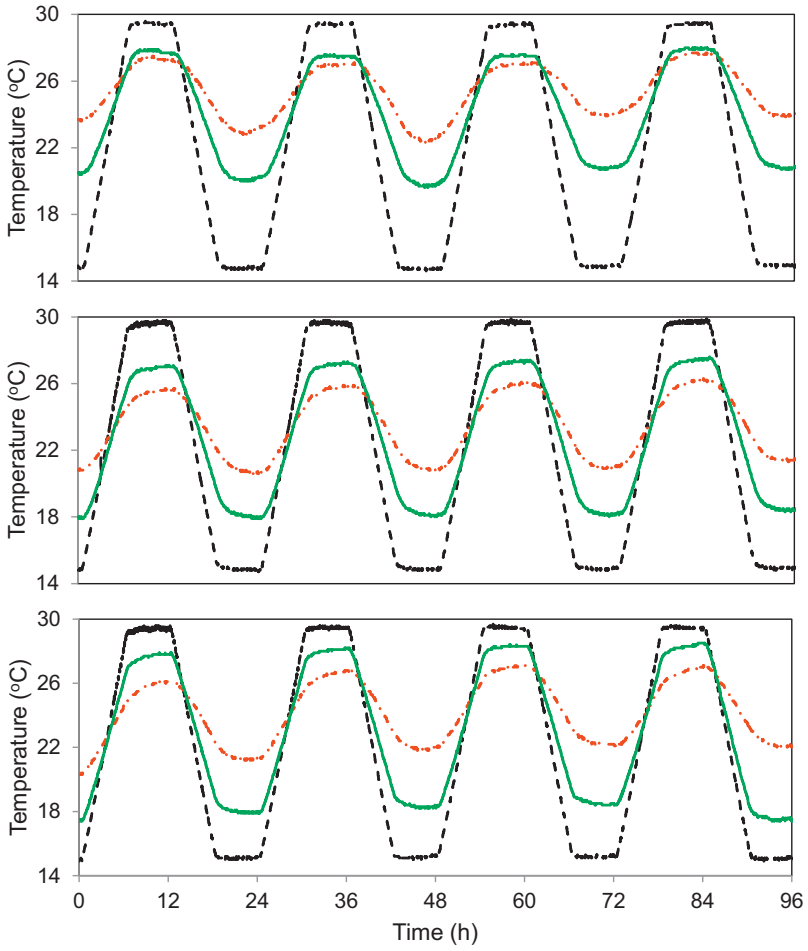


Fig. 10. Temperatures Tse (black dashed line), Tint (green solid line) and Tsi (red dot-dashed line) for the three ETIC systems; corn pith (top), wood (middle) and polystyrene (bottom) for 4 cycles (temperature shift from 15 to 30 °C and RH from 80% to 32%). (For interpretation of the references to colour in this figure legend, the reader is referred to the web version of this article.)

As it has been previously stated, each cycle consisted in a daily simultaneous variation of temperature and RH with the aim to simulate the evolution of outside weather conditions of an average spring day in a moderate climate. Thus, air temperature and RH within the chamber were comparable to the outside of a building while air conditions at the testing room were comparable to the inside of a building. The temperature at various positions, as well as the heat flux were reported all along the experiment.

The results of the tests are presented in Fig. 10. The temperatures at the surface inside the chamber (Tse), at the interface of the two insulation layers (Tint) and at the surface outside the chamber (Tsi) are plotted for 4 cycles. The results show a similar behaviour for the three insulation systems. However, minor differences are noted. Despite being the prototype with the largest total transmittance U, the temperature amplitude Tsi is lower in the wood system than in the polystyrene system (which has the lowest transmittance U). The attenuation factor (μ_{TI}), calculated as the ratio of the interior and exterior temperature amplitudes, was 0.33 for CA and WW and 0.37 for EPS (average of six consecutive cycles). Lower values indicate higher thermal inertia. As it was observed in previous tests for the WW boards alone (Section 3.3), in the wood system the sinusoidal shape of the curves is flattened. This indicates that the temperature change is slowed down when the temperature in the climate chamber is maintained. For the heat flux evolutions, similar results were obtained for the three systems.

From the results of this section, it can be concluded that the differences observed in the dynamic hygrothermal behaviour of the bio-based insulation boards compared with polystyrene are smaller in the ETIC systems. One of the reasons is probably the effect of the Portland cement mortar, which hinders the hygrothermal behaviour of the bio-based materials. Some new preliminary tests (not yet published) comparing different renders seem to support this assumption.

4. Conclusions

In this work, two bio-based insulation boards, corn pith and alginate (CA) and wood wool (WW), are compared with expanded polystyrene foam (EPS). EPS presents the lower thermal conductivity (0.036 W/mK), while the thermal conductivities of CA and WW insulators are in the same range, 0.042 and 0.048 W/mK respectively. Similarly, the thermal diffusivity values of both bio-based insulation boards are comparable: 0.70×10^{-6} m^2/s for CA and 0.76×10^{-6} m^2/s for WW, while EPS exhibits a significantly higher diffusivity of 2.1×10^{-6} m^2/s. Lower values of thermal diffusivity are related with a higher thermal inertia of the material.

Dynamic Vapour Sorption (DVS) results show that EPS adsorbs and desorbs less water vapour than bio-based materials. Furthermore, EPS sorption process is very fast. In the range of HR between

32% and 80 the variations in water vapour content are about 15% for CA, 7% for WW and 5% for EPS.

The results of the dynamic hygrothermal test show that when subjected to cyclic changes in temperature and humidity, the bio-based materials (WW and CA) experience a slower temperature change at the core of the sample than EPS. This behaviour can be explained due to the higher thermal inertia and hygroscopicity of the bio-based insulation boards. Moreover, distinct patterns were observed in the way the temperature changed in WW and CA, which is related to the difference in water absorption and desorption mechanisms found in DVS. In CA the variations of temperature and mass with the time are more gradual and more time is required to reach the final temperature and mass than in the WW.

Finally, the insulation boards were integrated in three ETIC systems, which contained two layers of insulation material and a render. In the case of the bio-based materials the second insulation layer was of higher density and therefore the thermal conductivities of the second layer were also higher. From the parameters obtained in the stationary thermic test the thermal resistances and transmittances of the system were worked out. As expected the ETIC system incorporating polystyrene had the lowest transmittance, 0.45 W/m^2K and the one incorporating wood, the highest: 0.61 W/m^2K.

The ETIC systems do not exhibit as remarkable differences as the insulation boards alone did in the dynamic hygrothermal test. The use of a render based on Portland cement mortar that diminishes breathability and therefore makes more difficult the water absorption and desorption processes may be one of the reasons to explain this fact. Other kind of renders more suitable for hygroscopic insulation materials (such as lime or earth-based mortars) should be investigated to elaborate bio-based ETIC systems.

Acknowledgements

This work was funded by MINECO (Spain) and AEI/FEDER/UE under the projects BIA2014-52688-R, BIA2017-88401-R and ENE2015-64117-C5-3-R. The authors would like to thank the Catalan Government for the quality accreditation given to their research group (2017 SGR 1758). M.P. would like to thank the Brazilian Education Ministry for the financial support received under the PNPD/Capes fellowship. This article has been possible with the support of the Ministerio de Economía y Competitividad (MINECO) and the Universitat Rovira i Virgili (URV) (FJCI-2016-28789).

References

[1] J. Carmeliet, H. Hens, S. Roels, O. Adan, H. Brocken, R. Cerny, et al., Determination of the liquid water diffusivity from transient moisture transfer experiments, J. Build. Phys. 27 (2004) 277–305, doi:10.1177/1097196304042324.
[2] F. Collet, J. Chamoin, S. Pretot, C. Lanos, Comparison of the hygric behaviour of three hemp concretes, Energy Build 62 (2013) 294–303. http://dx.doi.org/10.1016/j.enbuild.2013.03.010.
[3] F. Collet, S. Pretot, Thermal conductivity of hemp concretes: variation with formulation, density and water content, Constr. Build. Mater. 65 (2014) 612–619, doi:10.1016/j.conbuildmat.2014.05.039.
[4] A. Dowling, J.A. Mathias, Experimental determination of the insulating ability of corn by products, J. Sustain. Agric. 30 (2007) 15–27.
[5] M. Jerman, R. Cerny, Effect of moisture content on heat and moisture transport and storage properties of thermal insulation materials, Energy Build. 53 (2012) 39–46, doi:10.1016/j.enbuild.2012.07.002.
[6] M. Jerman, M. Keppert, J. Výborný, R. Černý, Hygric, thermal and durability properties of autoclaved aerated concrete, Constr. Build. Mater. 41 (2013) 352–359, doi:10.1016/j.conbuildmat.2012.12.036.
[7] A. Karamanos, S. Hadiarakou, A.M. Papadopoulos, The impact of temperature and moisture on the thermal performance of stone wool, Energy Build. 40 (2008) 1402–1411, doi:10.1016/j.enbuild.2008.01.004.
[8] A. Korjenic, V. Petránek, J. Zach, J. Hroudová, Development and performance evaluation of natural thermal-insulation materials composed of renewable resources, Energy Build. 43 (2011) 2518–2523.
[9] M.V. Madurwar, R.V. Ralegaonkar, S.A. Mandavgane, Application of agro-waste for sustainable construction materials: a review, Constr. Build. Mater. 38 (2013) 872–878.
[10] F. Ochs, W. Heidemann, H. Müller-Steinhagen, Effective thermal conductivity of moistened insulation materials as a function of temperature, Int. J. Heat Mass Transf. 51 (2008) 539–552, doi:10.1016/j.ijheatmasstransfer.2007.05.005.
[11] O.F. Osanyintola, C.J. Simonson, Moisture buffering capacity of hygroscopic building materials: experimental facilities and energy impact, Energy Build. 38 (2006) 1270–1282. http://dx.doi.org/10.1016/j.enbuild.2006.03.026.
[12] M. Palumbo, A.M. Lacasta, N. Holcroft, A. Shea, P. Walker, Determination of hygrothermal parameters of experimental and commercial bio-based insulation materials, Constr. Build. Mater. 124 (2016) 269–275. http://dx.doi.org/10.1016/j.conbuildmat.2016.07.106.
[13] M. Palumbo, Contribution to the Development of New Bio-Based Termal Insulation Materials Made from Vegetal Pith and Natural Binders, Universitat Politècnica de Catalunya, 2015 http://tdx.cat/handle/10803/314580.
[14] M. Palumbo, J. Formosa, A.M. Lacasta, Thermal degradation and fire behaviour of thermal insulation materials based on food crop by-products, Constr. Build. Mater. 79 (2015) 34–39.
[15] M. Palumbo, A.M. Lacasta, A. Navarro, M.P. Giraldo, B. Lesar, Improvement of fire reaction and mould growth resistance of a new bio-based thermal insulation material, Constr. Build. Mater. 139 (2017) 531–539.
[16] J. Pinto, A. Paiva, H. Varum, A. Costa, D. Cruz, S. Pereira, L. Fernandes, P. Tavares, J. Agarwal, Corn's cob as a potential ecological thermal insulation material, Energy Build. 43 (2011) 1985–1990.
[17] J. Pinto, B. Vieira, H. Pereira, C. Jacinto, P. Vilela, A. Paiva, S. Pereira, V.M.C.F. Cunha, H. Varum, Corn cob lightweight concrete for non-structural applications, Constr. Build. Mater. 34 (2012) 346–351.
[18] M. Qin, G. Walton, R. Belarbi, F. Allard, Simulation of whole building coupled hygrothermal-airflow transfer in different climates, Energy Convers. Manag. 52 (2011) 1470–1478. http://dx.doi.org/10.1016/j.enconman.2010.10.010.
[19] C. Rode, R. Peuhkuri, K.K. Hansen, B. Time, K. Svennberg, J. Arfvidsson, et al., Nordest project on moisture buffer value of materials, AIVC Conf. Energy Perform. Regul., 2005.
[20] C. Rode, R. Peuhkuri, B. Time, K. Svennberg, T. Ojanen, P. Mukhopadhyaya, et al., Moisture buffer value of building materials, J. ASTM Int. 4 (2007) 100369, doi:10.1520/JAI100369.
[21] C.J. Simonson, M. Salaonvaara, T. Ojanen, Heat and mass transfer between indoor air and a permeable and hygroscopic building envelope: Part II – Verification and numerical studies, J. Build. Phys. 28 (2004) 161–185. http://dx.doi.org/10.1177/1097196304044397.